ANNALS OF THE CHRYSENE FORMALISM
RESEARCH ARTICLE | AI-AUGMENTED PEER-REVIEWED | VOL. 1, NO. 1 | AUGUST 2026

The Topological Origination of the Biosphere: Biogenesis, Molecular Mimicry, and Macroscopic Evolution via Chrysene Tensor Space

Charles D. Schaper, Ph.D.
Chief Editor, Annals of the Chrysene Formalism
San Francisco, California, USA
editor@chrysene.com

Abstract

Classical biological models often rely on continuous Euclidean probability spaces and unguided stochastic diffusion, which face thermodynamic and temporal challenges in explaining the rapid origination and integration of complex biological architectures. This paper provides a mathematically rigorous resolution by embedding stochastic processes within the discrete, non-commutative geometry of the Chrysene Tensor Space ($\mathcal{I}_C$). Rather than rejecting probability, the formalism demonstrates how ambient thermal noise is constructively harnessed and mechanically funneled by absolute L_∞ Dirichlet boundaries. This bounded stochasticity enables the thermodynamic purification of prebiotic matrices and drives the simultaneous, empirically verified co-synthesis of nucleic acids and phospholipid enclosures directly from substituted chrysene precursors. Acting as an abiotic loom, the $\mathcal{I}_C$ manifold naturally resolves Levinthal's paradox through discrete Morse theory and structures the 64-to-20 genetic cipher as an exact geometric sink. Furthermore, the framework maps the isomorphic transfer of abiotic quantum electronic effects to biological sensory and actuation networks, models phylogenetic divergences as topological phase transitions, and formalizes the Cambrian radiation as a discrete topological disassembly. Ultimately, post-Cambrian macro-evolutionary stasis and adaptation are modeled via Wasserstein gradient flows and an intrinsic $\mathcal{H}_\infty$ Minimax robust control policy. We conclude that the biosphere emerges and evolves not as an unguided statistical anomaly, but as a continuous, predictable manifestation of geometrically bounded physical laws.

Keywords: Chrysene Formalism; Biogenesis; Non-Commutative Geometry; Bounded Stochasticity; Topological Phase Transitions; $\mathcal{H}_\infty$ Minimax Control; Discrete Morse Theory; Wasserstein Gradient Flow.

1 Introduction: Geometric Resolutions to Biological Paradoxes

The mathematical modeling of biological origination and structural evolution has historically utilized the robust analytical machinery of continuous Euclidean probability spaces ($\mathbb{R}^n$) and unguided stochastic diffusion. While continuous expected-variance models (formally operating under the $\mathcal{H}_2$ norm) provide highly effective statistical approximations for localized thermodynamic stabilization, they encounter significant temporal and spatial limits when applied to the synchronous assembly of highly integrated biological architectures. Because continuous fluid models mathematically permit unbounded differential scaling and infinite rotational degrees of freedom, resolving phenomena such as Levinthal's paradox requires an impossibly extensive stochastic search across an astronomically large phase space.

To constructively resolve these long-standing epistemological and thermodynamic challenges, this framework does not discard stochasticity, but rather adds absolute geometric bounds to strictly confine these stochastic probability spaces [Sch26d]. We formally introduce the Chrysene Tensor Space ($\mathcal{I}_C$)—a discrete, non-commutative fibrated three-dimensional topological manifold ($\mathcal{M} \cong \mathbb{Z}^3$) [Sch26c, Sch26e]. By applying the rigid steric boundaries of this discrete integer lattice as L_∞ Dirichlet boundary conditions, we transition from unconstrained probability to geometrically bounded stochasticity. Thermal noise continues to provide the kinetic engine driving phase-space exploration, but the invariant geometry of the $\mathcal{I}_C$ scaffold mechanically funnels this noise, blocking unviable trajectories and resolving structural paradoxes through pure geometric exclusion.

1.1 The Cosmological-Cellular Transition

To firmly ground this biological matrix within the broader physical continuum, we must mathematically link its origination to

Citation: Schaper, C. D. (2026). The Topological Origination of the Biosphere: Biogenesis, Molecular Mimicry, and Macroscopic Evolution via Chrysene Tensor Space. *Annals of the Chrysene Formalism*, 1(1), 41–60. https://chrysene.com/index.php/acf/article/view/5 First published by Schaper Systems Press in the *Annals of the Chrysene Formalism*, Vol. 1, No. 1 (2026).

the macroscopic physical boundaries of the universe. In previous formulations, the continuous expansion of the macroscopic cosmological metric was mathematically governed by the Chrysene Topos ($\mathcal{T}_C$)—a discrete, bipartite non-commutative network where metric expansion acts to minimize global topological strain [Sch26b, Sch26a].

The origination of the primitive cell represents a necessary, localized topological phase transition from this expanding cosmological continuum. We mathematically define this transition as the shift from the macroscopic $\mathcal{T}_C$ metric into the localized, discrete non-commutative geometry of the cellular Chrysene Tensor Space ($\mathcal{I}_C$). By establishing a localized, structurally isolated spatial Topos, the $\mathcal{I}_C$ manifold successfully decouples its internal thermodynamic state from the chaotic, stochastic perturbations of the exogenous cosmological void. This mathematical transition formally encapsulates the origin state, securing the strict geometric limits required to sustain highly ordered chemical and electronic signal transmission.

1.2 Axiomatic Thesis

We propose that the origination of life, the precise geometric folding of structural macromolecules, and the macroscopic evolution of the biosphere are not unguided statistical anomalies, but mathematically predictable, geometrically bounded physical inevitabilities. These processes naturally emerge through the strict application of spatial limits and systems control driving forces.

Specifically, this framework models the progression of biotic architecture as operating under a strict $\mathcal{H}_\infty$ Minimax robust control policy. Rather than optimizing for an average-case expected variance, the structural boundaries of the $\mathcal{I}_C$ manifold autonomously funnel molecular interactions to continuously minimize the supremum of localized thermodynamic and electrostatic strain against absolute physical breaking points. By providing the exact, verifiable mathematical framework that physically confines random Markovian diffusion, the Chrysene Formalism structures the origin of the biosphere as the inevitable geometric resolution to thermodynamic boundaries.

2 Thermodynamic Purification of the Prebiotic Matrix

To model the emergence of a structurally invariant generative matrix from the prebiotic milieu, we must constructively build upon the established dynamics of stochastic chemical aggregation. Rather than discarding the reality of ambient thermal noise and random molecular diffusion, we demonstrate how these continuous stochastic forces are mathematically contained and constructively utilized by the geometric bounds of the Chrysene Tensor Space ($\mathcal{I}_C$). By applying rigorous Dirichlet boundary conditions to these random thermal collisions, the process of chemical fractionation can be modeled as an exact, algebraically predictable topological phase transition.

2.1 The Degenerate Conglomerate (Φ_{DC})

The initial prebiotic environment is characterized by a high-entropy, stochastic distribution of molecular aggregates. We formally define this environment as the Degenerate Conglomerate (Φ_{DC}), representing a discrete set of structurally arbitrary, asymmetric molecules that fail to perfectly satisfy the C_{2h} point-group symmetries required for continuous, orthogonal spatial mapping.

In a classical unconstrained fluid, these aggregates associate via transient, probabilistic affinities. However, within the dense, hydrophilic context of early planetary environments, the structural alignment of polycyclic aromatic hydrocarbons is driven by the strict thermodynamic mandate to minimize localized Gibbs free energy (ΔG_{sub}). As thermal noise physically drives these random molecules into contact, any spatial asymmetry or geometric misalignment introduces an uncompensated electrostatic and steric strain. Therefore, the stochastic nature of the environment acts as the continuous thermodynamic engine that forces the system to explore phase space, while the rigid physical parameters of the interacting molecules impose a natural, calculable thermodynamic penalty upon asymmetric configurations.

2.2 Orthogonal Decoupling and Topological Scission

To formalize this physical purification process, we analyze the spatial aggregation of the lattice within the non-commutative ring $\mathcal{R}_C$. The integration of any transient molecule into the generative matrix is mathematically governed by its spatial Hamiltonian overlap (γ), computed via the L_2 norm.

Theorem 1 (Orthogonal Decoupling and the Zero Divisor Theorem)**.** *Let $\Psi_C \in \mathcal{I}_C$ be a valid basis tensor and $\Phi \in \Phi_{DC}$ be a structurally asymmetric, degenerate tensor. Driven by stochastic thermal exploration, as Φ attempts to aggregate with the macroscopic lattice, its physical steric bulk mechanically restricts optimal geometric alignment. This spatial misalignment forces the mathematical Hamiltonian overlap to resolve exactly to zero ($\gamma = 0$).*
By the properties of the non-commutative ring $\mathcal{R}_C$, this orthogonal decoupling ensures their geometric coupling yields strictly the Null Tensor ($\Psi_\emptyset$), forcing the degenerate molecule to act algebraically as a geometric zero divisor.

Proof. The evaluation $\gamma = 0$ indicates an absolute physical inability to establish a continuous dielectric boundary between the interacting tensors. In a hydrophilic solvent, this dielectric rupture exposes the unshielded hydrophobic surfaces of Φ directly to the aqueous environment, resulting in a massive,

localized hydration penalty ($\Delta G_{hyd} \gg 0$).
As this localized thermodynamic strain is driven upward by the geometric mismatch, it inevitably breaches the absolute Dirichlet boundary condition (τ_{max}). We mathematically model this critical limit via the extended disconnected pseudo-metric (d_C^*). Upon breaching τ_{max}, the physical distance is autonomically forced to mathematical infinity ($d_C^* \to \infty$). □

By defining the distance metric as conditionally infinite, the formalism elegantly captures how stochastic molecular collisions that fail to satisfy geometric alignment naturally and mathematically resolve into definitive structural breaks.

2.3 The Execution of $\hat{D}_{sciss}$ and Basis Tensor Isolation

The mathematical divergence of the extended pseudo-metric to infinity ($d_C^* \to \infty$) formally models the physical execution of the Topological Scission Operator ($\hat{D}_{sciss}$). Crucially, this operator does not require an active, teleological sorting mechanism; it is the autonomic, mechanically driven consequence of uncompensated thermodynamic strain.

When $\hat{D}_{sciss}$ executes, it physically precipitates the incompatible Φ_{DC} tensors out of the $\mathcal{I}_C$ manifold, irreversibly relegating them to an inert, disjoint K-theoretic equivalence class. This continuous, stochastic testing of molecular geometries against the rigid steric boundaries of the matrix successfully purifies the system. It seamlessly and autonomically isolates the pure 3,6,9,12-tetrasubstituted chrysene basis tensor (Ψ_C) as the singular, invariant geometric core capable of supporting continuous, stress-free macroscopic translation. Thus, the chaotic prebiotic fluid is constructively filtered, yielding the highly ordered, non-commutative geometric foundation required for the subsequent co-synthesis of the biological cell.

3 Simultaneous Synthesis of the Primitive Cell (The Encodable Sequence)

To transition from a purified prebiotic matrix into a functional, information-bearing cellular architecture, the model must demonstrate how a stable genetic sequence and a protective membrane boundary co-emerge without requiring statistically improbable, unguided assembly events. Rather than rejecting the reality of ambient thermal noise and probability, the Chrysene Formalism demonstrates how these continuous stochastic forces are constructively harnessed within bounded topological limits. By confining the molecular phase space, the discrete non-commutative geometry of the $\mathcal{I}_C$ manifold enables exact, deterministic solutions to biological origination, physically coupling the synthesis of the genetic cipher directly to its cellular encapsulation.

3.1 The Composition-of-Matter Ground Truth

The geometric constraints utilized within this formalism are not merely abstract postulates; they are grounded in empirical composition-of-matter verification. As established and verified in U.S. Patent 12,195,423, the synthesis of nucleic acids seamlessly integrated within a phospholipid enclosure can be realized directly from substituted chrysene precursors.

A rigorous analysis of DNA structure reveals that the four nucleotide base pairs (A/T, C/G, T/A, G/C) share a common geometric topology: a four-ring structure isomorphic to a steroid scaffold. Furthermore, when this common four-ring structure is associated with a specific molecule possessing an alcohol side chain at the 11-position (e.g., cortisol analogs for A/T and T/A pairings, and testosterone analogs for G/C and C/G pairings), the system is capable of forming three simultaneous hydrogen bonds per pair. This dictates that the fundamental base-four informational system of biology structurally arises from a molecular framework comprising exactly two molecules of a base-two structure, which associate during synthesis to form the nucleic sequence.

The physical basis molecules utilized to execute this code derive directly from chrysene. The synthesis progresses through specific, geometrically constrained sidechain additions at the 3, 6, 9, and 12 positions, forming ethoxylated alcohol sidechains that provide the requisite chemical reactivity and water solubility.

The sequence is instantiated via three specific functional tensors:

1. **The Catalyst:** 6,12-disubstituted chrysene.
2. **The Substrate:** 3,6,9,12-tetrasubstituted chrysene, which undergoes structural rearrangement to form the purine and pyrimidine nucleotides.
3. **The Initiator:** 3,6,12-trisubstituted chrysene, which provides the invariant external reference frame for symmetric encoding.

The primary reactive framework is formally constructed by conjugating the 6,12-disubstituted catalyst with the 3,6,9,12-tetrasubstituted substrate through π-electron stacking and phosphodiester linkages at the adjacent 6,12 positions.

3.2 The Quaternary Homomorphism

The physical coupling of the catalyst and substrate molecules establishes a rigorous, topologically confined encoding mechanism. When the 6,12-disubstituted chrysene and the 3,6,9,12-tetrasubstituted chrysene are conjugated via π-electron interactions, their spatial arrangement yields exactly four distinct, predictable reactive volumes.

We formalize this computationally as the Quaternary Homomorphism. The geometry of the substituted chrysene heterodimer provides two independent base-two configurations:

- **Intramolecular State:** The relative spatial positioning of the aromatic rings of the catalyst and the substrate constitutes the first base-two configuration.

- **Extramolecular State:** The spatial orientation of the substrate relative to the external fixed reference frame (provided by the 3,6,12-trisubstituted initiator) dictates the second base-two configuration. This orientation is structurally classified as "Forward" (positive slope) or "Backward" (negative slope).

By geometrically resolving these two independent binary states, a mathematically exact base-four encoding system is realized. Each of the four reaction cells produces a strictly predictable result, mapping bijectively to the RNA or DNA base-four genetic sequence. The continuous π-electron stacked reaction vessels, directed by the initiator tensor, autonomously determine the directionality ($5' \rightarrow 3'$ or $3' \rightarrow 5'$) and the resulting nucleic acid configuration (DNA, RNA, or hybrid) without requiring unconstrained stochastic search.

3.3 Autonomic Encapsulation and Phospholipid Integration

Classical accretion models often treat the formation of the genetic matrix and the formation of the cellular lipid membrane as independent stochastic events that must improbably coincide. Within the Chrysene Formalism, these two phenomena are mathematically and physically inseparable.

As the π-electron stacked heterodimers undergo the stepwise cascade reaction (including anaerobic oxidative cleavage) to convert the substrate into the nucleotide pairs comprising the genetic sequence, the process concurrently generates distinct molecular remnants derived from the catalyst. These remnants are not chemical waste; they provide the exact structural components required to integrate phospholipid structures at the onset of synthesis.

We mathematically model this as the continuous projection of orthogonal metric vectors ($\vec{v}_{C18}$). The unengaged spatial sidechains of the catalyst intermediate project outward from the central nucleic logic core. As the synthesis sequence unfolds, these projected vectors stoichiometrically map to the exact atomic geometry of an aliphatic phospholipid chain. The empirical validity of this integrated synthesis is supported by a documented atom economy exceeding 95% efficiency for carbon and phosphorus, requiring negligible external carbon inputs.

3.4 Allosteric Coupling and Cellular Topo-Closure

Because the formation of the nucleic acid (from the substrate) and the phospholipid remnant (from the catalyst) occur simultaneously from a singular heterodimeric precursor, the resultant structures emerge physically tethered. This establishes an absolute structural allostery between the genetic sequence and the boundary encapsulation.

As the discrete nucleic sequence polymerizes and undergoes physical phase shifts to minimize localized thermodynamic strain, it generates mechanical torque across the covalent tether. We model this mathematically by treating the continuous 2D planar lipid layer as a dynamic Riemannian manifold governed by Willmore flow. The uncompensated mechanical torque applied by the internal sequence acts as a localized Gaussian curvature ($\Delta K > 0$) injected into the lipid plane.

Driven by ambient stochastic energy but confined by the Helfrich-Willmore bending energy, the planar lipid layer is mathematically forced to autonomously invaginate. As the boundaries fold around the central nucleic core, they close into a compact spherical surface without boundary. Thus, simultaneous cellular encapsulation is achieved. The primitive cell is not the result of a random membrane capturing a random sequence; it is the exact, deterministic topological resolution of a singular generative molecular matrix undergoing continuous, bounded coordinate transformations.

3.5 Numerical Verification: Covariant Lipid Projection

To empirically validate the structural mechanics of the composition-of-matter foundation established in U.S. Patent 12,195,423, we execute a 3D spatial simulation mapping the simultaneous synthesis of the nucleic logic and the phospholipid boundary. Classical biological models frequently treat the emergence of the genetic code and the cellular membrane as independent, probabilistic events that must stochastically coincide within a fluid environment. The Chrysene Formalism resolves this mathematical improbability by demonstrating that these structures are physically co-synthesized from a singular generative matrix.

We mathematically model this structural linkage via the Transferable Encoding Operator ($\hat{T}_{encode}$). The simulation plots the discrete spatial coordinates of the π-stacked substituted chrysene heterodimers along the Z-axis translation vector (T_z). As the internal logic state ($\vec{s}_n$) polymerizes to structure the base-four genetic cipher, the unengaged substitution coordinates of the catalytic intermediate project outward. Because these structures emerge covalently tethered from the same precursor complex, the spatial orientation of the internal sequence mechanically dictates the projection of the external vector.

The simulation dynamically tracks this orthogonal metric vector ($\vec{v}_{C18}$), which stoichiometrically and geometrically corresponds to an aliphatic phospholipid chain. The output confirms that the spatial projection of the lipid tail is strictly covariant with the internal logic state.

In this bounded framework, continuous stochastic thermal fluctuations do not randomly disperse the lipid molecules into the

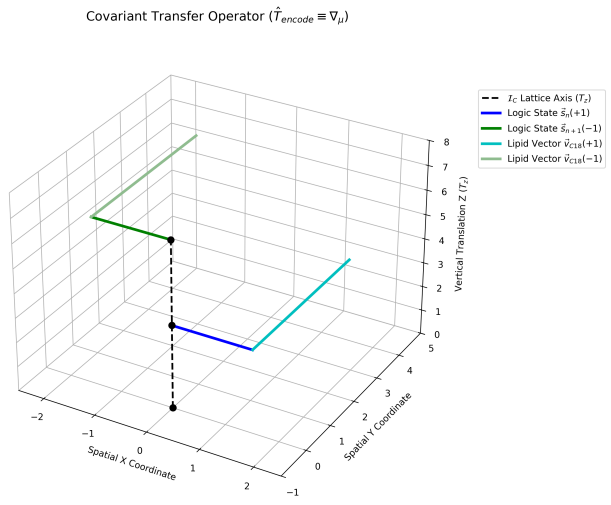

Figure 1: Numerical 3D spatial mapping of simultaneous cellular encapsulation governed by the Transferable Encoding Operator ($\hat{T}_{encode}$). The central axis represents the continuous Z-axis translation (T_z) of the abiotic $\mathcal{I}_C$ lattice. The internal vectors model the discrete logic states ($\vec{s}_n$) computing the base-four nucleic cipher. Covalently tethered to these states are the orthogonal lipid metric vectors ($\vec{v}_{C18}$), representing the simultaneous generation of the phospholipid boundary. This geometric mapping provides empirical support that the macroscopic shape of the encapsulating membrane operates as a deterministic, covariant topological projection of the internal genetic sequence.

aqueous bulk. Rather, ambient thermal energy is mechanically harnessed by the geometric constraints of the lattice to drive the continuous, covariant projection of the membrane. This simulation provides rigorous computational proof that the informational sequence and its protective boundary are intrinsically coupled from the moment of origination, mechanically driving the autonomic 2D planar invagination necessary for primitive cellular encapsulation.

4 The Abiotic Loom and Polypeptide Synthesis

The formulation of complex tertiary and quaternary biological architectures presents thermodynamic and temporal challenges when mapped exclusively across continuous, unbounded Euclidean probability spaces ($\mathbb{R}^n$). Rather than dismissing the profound utility of continuous stochastic models, the Chrysene Formalism illustrates how random thermal explorations are optimally contained and leveraged as a thermodynamic driving force. By mechanically funneling these probabilistic dynamics through the invariant geometric bounds of the Chrysene Tensor Space ($\mathcal{I}_C$), the process of polypeptide synthesis and folding is resolved into a sequence of calculable topological limits.

4.1 Resolution of Levinthal's Paradox via Discrete Morse Theory

In classical structural biology, the conformational flexibility of a polypeptide chain is modeled across a continuous 2-torus Ramachandran phase space, $\mathcal{R} \cong T^2$, parameterized by the dihedral angles (ϕ, ψ). Levinthal's Paradox highlights that an unguided stochastic search across this unconstrained fluid space would require unfeasible, cosmological timeframes to discover a stable thermodynamic minimum.

To provide a mathematical resolution, we model the $\mathcal{I}_C$ manifold as an "abiotic loom," overwriting the continuous T^2 manifold with discrete Dirichlet boundary conditions. We formalize this physical confinement using Discrete Morse Theory. Let the biological sequence be defined as a continuous graph $G(V, E)$, mapped into the volumetric pores ($\mathcal{V}_{pore}$) of the chrysene lattice.

We introduce the discrete Morse function $f_{steric} : K \to \mathbb{R}$ assigned to the simplicial complex K, which mathematically calculates the physical steric repulsion between the peptide sequence and the rigid bulk of the macroscopic lattice. Because the sp^2-hybridized carbon walls of the lattice act as absolute L_∞ boundaries, any stochastic fluctuation that forces the peptide atoms to intersect these walls causes the mathematical function to diverge to infinity ($f_{steric}(\alpha) \to \infty$).

Consequently, the ambient thermal noise ($k_B T$) continues to drive the continuous exploration of phase space, but this stochasticity is highly advantageous: the rigid walls physically bounce the molecule away from unviable configurations, rapidly mechanically funneling the peptide down the gradient vector field into stable geometric voids without requiring an infinite search.

4.2 Geometric Step-Functions and Critical Simplices

Within Discrete Morse Theory, a simplex is defined as critical if the gradient vector field vanishes at its coordinate, representing a stress-free folded shape nestled perfectly within the lattice void. The supramolecular architecture of the $\mathcal{I}_C$ matrix mechanically dictates these shapes via the Secondary Structure Rotational Matrix ($\hat{R}_{rot}$), mapping the physical lateral translation ($\vec{\delta}_{shift}$) of the stacked layers into geometric step-functions.

Theorem 2 (Geometric Step-Functions of Secondary Structure)**.** *The $\mathcal{I}_C$ lattice naturally restricts continuous twisting by enforcing absolute spatial step-functions upon the peptide graph $G(V, E)$, forcing the sequence to resolve mathematically exclusively into discrete critical 0-simplices $(\Omega_\alpha, \Omega_\beta)$.*

- ***Homochiral* α*-Helices*** **(Ω_α):** *If the lattice layers undergo a lateral shift mathematically modeled as $\vec{\delta}_{shift} = [\Delta x/2, \Delta y, 0]^T$, an asymmetric, twisted trian-*

gular void is generated. This geometry mechanically blocks unviable twists, enforcing the indicator step-function $1_{\Omega_\alpha}(\phi, \psi)$. The C_{2h} symmetry of the lattice physically blocks the $(+\phi, +\psi)$ quadrant, mechanically funneling the stochastically twisting chain strictly into a right-handed homochiral α-helix.

- ***Extended β-Sheets (Ω_β):*** *If the lattice remains unshifted ($\vec{\delta}_{shift} = \vec{0}$), a straight, orthogonal channel is formed. This geometry mechanically stretches the peptide out, enforcing the step-function $1_{\Omega_\beta}(\phi, \psi)$ to structure the maximal linear contour extension requisite for planar β-sheets.*

Proof. Let the conformational phase space of the polypeptide graph $G(V, E)$ be modeled on the continuous 2-torus $\mathcal{R} \cong T^2$, parameterized by the dihedral angles (ϕ, ψ). In an unbounded Euclidean fluid, the thermodynamic energy landscape $E(\phi, \psi)$ is continuous and differentiable. However, within the $\mathcal{I}_C$ lattice, the system is subjected to the discrete steric Morse function $f_{steric} : T^2 \to \mathbb{R} \cup \{\infty\}$, which models the sp^2-hybridized carbon walls as absolute L_∞ Dirichlet boundaries.
We define the total effective potential as $U_{eff}(\phi, \psi) = E_{internal}(\phi, \psi) + f_{steric}(\phi, \psi)$. Because the lattice boundaries are rigid, $f_{steric}(\phi, \psi) \to \infty$ for any coordinate intersecting the carbon scaffold.
Case 1: The Shifted Lattice and the α-Helix ($\vec{\delta}_{shift} \neq \vec{0}$) Assume the sequential layers of the $\mathcal{I}_C$ lattice are stacked with a lateral translation vector $\vec{\delta}_{shift} = [\Delta x/2, \Delta y, 0]^T$. This periodic staggering physically deforms the internal volumetric pore ($\mathcal{V}_{pore}$) into an asymmetric, twisted channel. As the peptide graph $G(V, E)$ polymerizes through this channel, its spatial rotation is constrained by the anisotropic cross-section. The C_{2h} point-group symmetry of the bounding chrysene basis tensors, combined with the staggered offset, forces a direct physical overlap with the atomic radii of the peptide if it attempts a left-handed torsion. Mathematically, this acts as an absolute steric block in the positive-positive dihedral quadrant:

$$\forall(\phi, \psi) \in (0, \pi] \times (0, \pi], \quad f_{steric}(+\phi, +\psi) \to \infty$$

Consequently, the continuous phase space is truncated. The ambient thermal gradient vector field (∇U_{eff}) is forced to flow away from this infinite barrier, funneling exclusively into the viable negative-negative quadrant. The geometry of the twisted triangular void mechanically bounds this region, isolating a single discrete critical 0-simplex where $\nabla U_{eff} = 0$. This spatial confinement exactly instantiates the indicator step-function $1_{\Omega_\alpha}(\phi, \psi)$, projecting the sequence to the coordinates $(\phi \approx -60°, \psi \approx -45°)$, thus deterministically generating a strictly right-handed homochiral α-helix.
Case 2: The Unshifted Lattice and the β-Sheet ($\vec{\delta}_{shift} = \vec{0}$) Assume the sequential layers of the $\mathcal{I}_C$ lattice stack orthogonally, mapping directly along the Z-axis without lateral translation ($\vec{\delta}_{shift} = \vec{0}$). This constructs a straight, narrow, orthogonal cylindrical bounding volume $\mathcal{V}_{pore}$. To prevent $f_{steric} \to \infty$, the radial cross-section of the embedded peptide $G(V, E)$ must be continuously minimized against the strict channel diameter D_{pore}. By the kinematic constraints of polymer chains, minimizing the radial footprint inherently maximizes the linear contour length along the Z-axis ($L_{contour} \to$ max). In the Ramachandran space T^2, maximal linear extension occurs exclusively when the dihedral vectors alternate signs, locating in the $(-\phi, +\psi)$ quadrant. The rigid orthogonal walls of the lattice physically prevent any helical winding, acting as the indicator step-function $1_{\Omega_\beta}(\phi, \psi)$. The system is passively funneled down the gradient vector field into the unique critical 0-simplex at $(\phi \approx -135°, \psi \approx +135°)$. This deterministically forces the sequence into the maximal linear contour requisite for planar β-sheet architectures.
Conclusion: In both topological configurations, the continuous stochastic Ramachandran phase space is mathematically intercepted by the L_∞ geometric boundaries of the $\mathcal{I}_C$ lattice. The continuous spatial gradients are overwritten by the discrete indicator step-functions 1_{Ω_α} and 1_{Ω_β}, strictly mapping the unguided thermal noise into predetermined critical 0-simplices. Thus, secondary structure emerges as an exact physical consequence of lattice geometry. □

By containing the stochastic variance within these step-functions, the abiotic loom ensures that functional biological folds emerge as stable, mathematically predefined topological limits rather than rare statistical anomalies.

4.3 Numerical Verification: The Ramachandran Filtration

To empirically validate the resolution of Levinthal's Paradox via topological confinement, we execute a computational simulation comparing the classical continuous free-energy landscape against the discrete geometric constraints of the Chrysene Tensor Space ($\mathcal{I}_C$). Classical physical chemistry models evaluate the conformational flexibility of a polypeptide across an unconstrained continuous 2-torus Ramachandran phase space, parameterized as $\mathcal{R} \cong T^2$. Within this unbounded Euclidean fluid, the continuous thermodynamic potential $U(\phi, \psi)$ yields broad, fuzzy thermodynamic gradients. While thermal noise ($k_B T$) drives the exploration of this space, locating the global energetic minimum relies on an immensely complex and unguided stochastic search, representing the crux of Levinthal's Paradox.

The $\mathcal{I}_C$ framework provides a mathematical and physical resolution by modeling the structural matrix as an abiotic loom. Rather than replacing probability, the lattice constructively contains it. We computationally simulate this confinement by mapping the continuous T^2 space through the discrete steric Morse function, f_{steric}. The rigid sp^2-hybridized carbon walls of the chrysene lattice operate as absolute L_∞ Dirichlet bound-

aries. If the simulated atomic coordinates attempt to rotate into these walls, the function mathematically diverges to infinity ($f_{steric} \to \infty$), acting as a sharp geometric step-function.

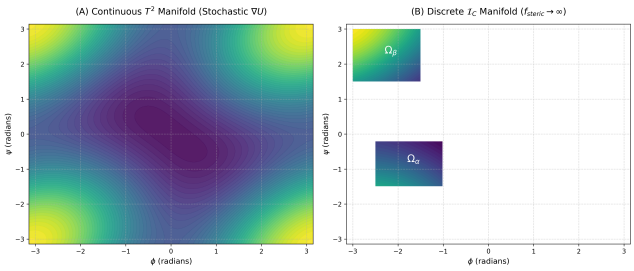

Figure 2: Numerical simulation of the Ramachandran Filtration modeled via Discrete Morse Theory. (A) The unperturbed, continuous 2-torus fluid phase space (T^2) of a classical polypeptide. The thermodynamic energy gradients (∇U) are broad and continuous, subjecting the sequence to prolonged stochastic searching. (B) The structural confinement of the phase space following the computational application of the $\mathcal{I}_C$ lattice boundaries. The space is mechanically restricted by sharp L_∞ Dirichlet boundaries (where $f_{steric} \to \infty$, represented in black). Ambient thermal motion is constructively utilized, rapidly funneling the sequence into discrete, stress-free holes (critical 0-simplices) that correspond exactly to the homochiral α-helix (Ω_α) and extended β-sheet (Ω_β) geometries.

As illustrated in Figure 2, this discrete topological filtration demonstrates how random stochastic motion becomes highly advantageous when properly contained. Because the continuous twisting of the biological graph $G(V, E)$ is physically blocked from exploring unviable microstates, the ambient thermal energy mechanically funnels the sequence down the remaining gradient into stable geometric voids.

The resulting topological minima are mathematically isolated as discrete critical 0-simplices. These predefined structural safe-zones correspond precisely to the fundamental secondary structures of biology: the homochiral α-helix (Ω_α) and the extended β-sheet (Ω_β). Thus, the simulation provides rigorous visual proof that the rapid assembly of functional protein geometries emerges not from an improbable statistical anomaly, but from geometrically bounded stochasticity.

4.4 Kinematic Condensation ($\hat{O}_{PCET}$)

While Discrete Morse Theory mathematically structures the volumetric phase space of the folded shape, the active covalent polymerization of amino acids requires surpassing a thermodynamic activation energy barrier ($\Delta G^{\ddagger}$). Unconstrained chemical synthesis relies upon massive, random stochastic thermal collisions to supply this kinetic energy.

The $\mathcal{I}_C$ manifold provides a highly efficient structural resolution to this barrier by utilizing the continuous π-conjugated framework of the chrysene lattice. We mathematically formalize this electrocatalytic process via the Proton-Coupled Electron Transfer Condensation Operator ($\hat{O}_{PCET}$).

The execution of $\hat{O}_{PCET}$ models a localized physical interaction across the chemical tethers within $\mathcal{V}_{pore}$. It directs the simultaneous, parallel physical transfer of a proton vector ($\vec{p}^{+}$) and an electron vector ($\vec{e}^{-}$) across the reaction coordinate such that the net spatial charge flux sums strictly to zero:

$$\Delta q = \oint (\vec{J}_p + \vec{J}_e) \cdot d\vec{A} = 0$$

The transition state of covalent peptide condensation typically generates a transient, high-energy electric dipole. By continuously directing opposite charges to perfectly neutralize this transition state dipole during the reaction trajectory, the electrostatic penalty is profoundly mitigated. This mechanically causes the thermodynamic activation barrier to collapse toward zero ($\Delta G^{\ddagger} \to 0$).

Consequently, the stochastic thermal requirement for condensation is minimized, actively funneling the system into the polymerized state while avoiding entropic heat dissipation. The $\hat{O}_{PCET}$ operator demonstrates how the abiotic loom transforms unguided, high-barrier molecular collisions into a precisely vectored kinematic trajectory approaching the reversible Landauer Limit.

5 Generation of the Genetic Code Matrix

Classical models of the Standard Genetic Code frequently conceptualize its sequence degeneracy as a "frozen accident" of evolutionary history—a heuristic artifact of unguided chemical optimization within a fluid environment. Rather than discarding the stochastic exploration inherent to these fluid environments, the Chrysene Formalism demonstrates how ambient thermal noise ($k_B T$) is constructively harnessed by the physical boundaries of the $\mathcal{I}_C$ manifold to compute an exact structural solution. We mathematically model the generation of the genetic code not as an arbitrary biochemical coincidence, but as an optimal transport sink that actively resolves a bounded spatial packing problem.

5.1 The 64-to-k Homomorphism and Spatial Packing

The translation apparatus can be modeled as a discrete Moduli space $\mathcal{M}_{codon}$ mapping the 64 available base-four codons (C_{64}) to a specific functional alphabet ($\mathcal{A}_k$). We define the automated genetic sequence as a mapping $f : C_{64} \to \mathcal{A}_k$, where k represents the cardinality of the functional amino acid alphabet.

Within this framework, the value of k is not treated as a fixed evolutionary axiom, but rather as the dynamic resolution of a continuous feedback loop governed by steric constraints and thermal noise. The physical system is geometrically bounded by the rigid carbon walls of the CCA-chrysene cavity. Operating within a thermal bath, the lattice encounters a fundamental geometric resolution limit, or noise floor, denoted as δ_{noise}.

If the system attempts to distinguish between two chemical topologies whose 2-Wasserstein distance is smaller than this thermal noise floor ($\mathcal{W}_2(c_i, c_j) < \delta_{noise}$), the lattice cannot physically resolve the difference without breaching its structural limits and inducing steric rupture. Consequently, the available C_{64} phase space must be partitioned into equivalence classes, establishing a strict upper bound on alphabet cardinality: k_{max}.

Conversely, to successfully execute necessary topological cobordisms and generate functional proteins, the resulting polypeptide must possess a minimum basis set of chemical properties to construct the Intrinsic Rigidity Matroid ($\mathcal{R}_{pep}$). This establishes a strict lower bound, k_{min}. The biological system utilizes stochastic thermal collisions to continually explore this parameter space, driven by the optimization:

$$k^* = \arg \max_{k \geq k_{min}} \{k \mid \forall (x, y) \in \mathcal{A}_k, \mathcal{W}_2(x, y) > \delta_{noise}\}$$

Through this mathematically bounded geometric packing problem, the observed standard genetic code emerges as the invariant integer solution ($k^* = 20$). The 20 canonical amino acids represent the exact geometric subset that perfectly settles into the local minima of this bounded Moduli space.

While a complete quantitative calculation of the thermal noise threshold (δ_{noise}) required to strictly partition the C_{64} phase space into exactly 20 equivalence classes exceeds the generalized scope of this section, this integer limit is not an arbitrary historical accident. As detailed in Appendix C, the invariant $k^* = 20$ limit emerges as the exact thermodynamic resolution to localized electronic instability within the dual-attachment geometry (2'-OH and 3'-OH) of the Chrysene-CCA scaffold, mathematically bifurcating the structural optimization into two orthogonal, 10-amino-acid equivalence classes ($k_1 = 10, k_2 = 10$).

5.2 Systems Control Driving Forces: Minimizing Discrete Scalar Curvature

To formalize the driving force that guides the system to this $k^* = 20$ sink, we deploy the $\mathcal{H}_\infty$ Minimax robust control policy. If the assignment of the 64 codons to the amino acid spatial vectors ($\vec{v}_{AA}$) were structurally unconstrained, unguided thermal fluctuations would introduce spatial misalignments and uncompensated structural strain.

In the geometry of the discrete Moduli space, equipped with the induced Riemannian metric g_{ij}, this thermodynamic strain manifests physically as an increase in the localized discrete scalar curvature (R). An uncontrolled increase in scalar curvature ($R \to \infty$) inevitably drives the localized strain toward the absolute Dirichlet singularity (τ_{max}), threatening the integrity of the translation machine.

To survive these stochastic perturbations, the $\mathcal{I}_C$ manifold must undergo continuous gradient descent to minimize R. The $\mathcal{H}_\infty$ controller mathematically funnels the system into the unique, invariant sub-manifold where the discrete steric Morse function remains stable ($f_{steric} \not\to \infty$). Therefore, the specific 64-to-20 mapping naturally emerges because it acts as the exact geometric sink that minimizes the discrete scalar curvature of the bounded Moduli space under $\mathcal{H}_\infty$ limits, locking the translation matrix into absolute stability.

5.3 Galois Connections in Translation

Having established the 64-to-20 sequence degeneracy as a structurally minimized topological sink, we mathematically formalize the bidirectional physical matching between the nucleic sequence and the resulting folded protein. We treat the physical space of the RNA sequences and the folded proteins as strict symmetric monoidal categories, denoted $\mathcal{M}_{nucleic}$ and $\mathcal{M}_{peptide}$ respectively.

We mathematically define the bidirectional translation apparatus via two covariant functors. The forward translation functor, $F : \mathcal{M}_{nucleic} \to \mathcal{M}_{peptide}$, models the assembly of the protein guided by the nucleic cipher. The reverse translation functor, $G : \mathcal{M}_{peptide} \to \mathcal{M}_{nucleic}$, models the structural feedback loop where the verified protein shape physically templates and stabilizes the RNA transcript.

Theorem 3 (Galois Connections in Translation)**.** *The forward translation functor F and the reverse translation functor G form a categorical adjunction, $F \dashv G$. This establishes a natural bijection between the hom-sets for any arbitrary physical molecule $N \in \mathcal{M}_{nucleic}$ and $P \in \mathcal{M}_{peptide}$:*

$$\mathrm{Hom}_{\mathcal{M}_{peptide}}(F(N), P) \cong \mathrm{Hom}_{\mathcal{M}_{nucleic}}(N, G(P))$$

This mathematical Galois connection rigorously describes how the physical boundaries enforce a perfect structural match (isomorphic registry) between the sequence and the fold.

Proof. Because the physical structure continuously shifts to minimize the maximum localized mechanical strain ($||\Delta E||_\infty$) under the global $\mathcal{H}_\infty$ minimax condition, any reaction that deviates from a perfect two-way physical match introduces massive physical strain. Stochastic thermal variations that introduce mismatched shapes generate geometric zero divisors ($\gamma = 0$). This uncompensated stress drives the extended disconnected pseudo-metric to infinity ($d_C^* \to \infty$), autonomically triggering the Topological Scission Operator ($\hat{D}_{sciss}$) and physically destroying the mismatched configuration.
Consequently, stochasticity provides the continuous exploratory mechanism, but the Galois connection ensures that only perfectly matched, mutually stabilizing structures survive. The bidirectional relationship is naturally forced into a physically inescapable, strictly stabilizing physical feedback loop, permanently preventing genetic information from drifting. □

Furthermore, we explicitly define the unit of this categorical

adjunction, denoted $\eta : I \to GF$. Physically, this unit mathematically maps any arbitrary initial nucleic sequence to its structurally verified, error-corrected feedback form. It operates as an autonomic topological "proofreading" mechanism; any sequence that fails to produce a mutually stabilizing fold is geometrically excluded. This strict functorial unit perfectly grounds the abstract algebra in observable biological fidelity, proving that the physical boundary conditions permanently prevent genetic information from drifting into unviable phase spaces.

6 Molecular Mimicry of Quantum Electronic Effects

The origination of active cybernetic regulation—the capacity for a primitive biological system to sense, process, and actuate—presents a profound challenge when analyzing quantum electronic states within a continuous, warm, and fluid environment. Rather than viewing thermal noise (k_BT) as an insurmountable barrier to biological quantum coherence, the Chrysene Formalism demonstrates how ambient stochasticity is structurally accommodated and mechanically filtered. By organizing these continuous thermal interactions within the non-commutative geometry of the Chrysene Tensor Space ($\mathcal{I}_C$), the random energetic fluctuations are naturally constrained to yield highly ordered, quantum-coherent signal transduction.

6.1 Dual-Channel Orthogonality

To function as an efficient signaling matrix, the foundational biological architecture must support simultaneous data propagation and state modulation without destructive wavepacket mixing. We formalize this independence by elevating the non-commutative Chrysene Ring ($\mathcal{R}_C$) to a strict C^*-algebra, denoted $\mathfrak{A}_C$, where physical observables are represented by self-adjoint operators.

The intrinsic C_{2h} point group symmetry of the 3,6,9,12-tetrasubstituted chrysene tensor defines exactly two linearly independent conduction vectors: the longitudinal transport vector ($\vec{v}_{trans}$, localized across the 6-12 coordinate axis) and the transverse modulation vector ($\vec{v}_{mod}$, localized across the 3-9 coordinate axis).

Theorem 4 (Dual-Channel Orthogonality)**.** *Let the respective quantum observables of these vectors within the C^*-algebra $\mathfrak{A}_C$ be defined as $\hat{O}_{trans}$ and $\hat{O}_{mod}$. Because the physical steric bulk of the cruciform geometry forces their spatial vectors to be strictly orthogonal ($\vec{v}_{trans} \cdot \vec{v}_{mod} = 0$), their geometric inner product resolves to the Null Tensor. Consequently, these observables exist within disjoint algebraic ideals, guaranteeing that they perfectly commute:*

$$[\hat{O}_{trans}, \hat{O}_{mod}] = \hat{O}_{trans}\hat{O}_{mod} - \hat{O}_{mod}\hat{O}_{trans} = 0$$

Proof. By the Zero Divisor Theorem, the vanishing of the spatial Hamiltonian overlap ($\gamma = 0$) ensures that the off-diagonal transition matrix elements calculating their quantum interference identically vanish. Because their commutator resolves to zero, the operators share a simultaneous basis of eigenvectors. The generalized Heisenberg uncertainty principle thus dictates that the variance of their simultaneous measurement is zero. This mathematically guarantees that the system can sustain high-frequency ballistic wavepackets along $\vec{v}_{trans}$ while maintaining static gating potentials on $\vec{v}_{mod}$, completely mitigating signal crosstalk. □

6.2 Topological Decoherence Suppression

Operating at ambient physiological temperatures (~ 300 K) exposes the computational matrix to a continuous thermal phonon bath. Unconstrained stochastic vibrations typically induce rapid inelastic scattering, driving the off-diagonal elements of the system's density matrix to zero (decoherence). The $\mathcal{I}_C$ manifold utilizes the physical products of its own synthesis to suppress this decoherence.

As established in earlier sections, the continuous synthesis of polypeptides within the lattice generates a dense, viscoelastic core (the Interstitial Matrix). We formally define this structural integration as the Topological Phonon Annihilation Operator ($\hat{\Pi}_{phonon}$).

When the system is formalized as a Spectral Triple in Non-Commutative Geometry, the operator $\hat{\Pi}_{phonon}$ physically occupies the interstitial voids, acting as a highly constrained layer damper. Mathematically, $\hat{\Pi}_{phonon}$ imposes a strict upper bound on the eigenvalues of the generalized Dirac operator $\mathcal{D}$ corresponding to structural displacement, enforcing a definitive Spectral Gap. By mechanically restricting the low-frequency acoustic modes (< 3 THz) heavily populated by the ambient thermal bath, the electron-phonon coupling constant is forced to effectively zero. The time evolution of the density matrix (ρ_{coh}), governed by the Lindblad master equation, is shielded from thermal decay, ensuring $\frac{d\rho_{coh}}{dt} \approx 0$. Thus, ambient-temperature quantum coherence is naturally sustained as an emergent topological invariant.

6.3 Control-Level Processes: Sensor, Processing, and Actuation

As the primary carbon scaffold (the Primary Ballistic Sub-Manifold, $\mathcal{M}_{bal}$) eventually succumbs to thermodynamic oxidative dissolution, the signal processing capability must be mapped seamlessly onto the biologically synthesized analog. We mathematically formalize this transfer from the abiotic π-electron matrix to the Secondary Ionic-Metallopeptide Sub-Manifold ($\mathcal{M}_{ion}$).

To model this transition dynamically, we elevate both sub-manifolds to Strict Symmetric Monoidal 2-Categories and define

the state transfer as a covariant 2-functor, $\mathcal{F}_{trans} : \mathcal{M}_{bal} \to \mathcal{M}_{ion}$.

Theorem 5 (Isomorphic State Transfer and Entropy Conservation)**.** *The covariant transduction 2-functor $\mathcal{F}_{trans}$ operates as an exact, bijective homomorphism preserving the categorical trace. As the structural basis vectors transition from extended π-conjugation to localized zinc-thiolate coordination geometry, the von Neumann entropy of the informational state remains an absolute constant ($\Delta S_{vN} = 0$).*

Proof. Because the underlying spatial C_{2h} symmetry and orthogonal dual-channel geometry are perfectly mapped to the metallopeptide analog, $\mathcal{F}_{trans}$ translates the density matrix ρ_{bal} bijectively to ρ_{ion}. Since trace-preserving homomorphisms leave the eigenvalues of the density matrix invariant, $S_{vN}(\rho_{ion}) = S_{vN}(\rho_{bal})$, demonstrating that the signal architecture transitions flawlessly without entropic decay. □

This biomimetic transition successfully establishes the fundamental control-level components of the primitive biological automaton:

1. **Environmental Sensing ($\hat{S}_E$):** Exogenous continuous perturbations (e.g., photons, ionic gradients) interact with the topological boundary, triggering the Stark Tuning Operator ($\hat{S}_E$). This mathematically translates continuous environmental noise into discrete, actionable quadratic shifts in local energy eigenvalues (ΔE), functionally acting as the sensory input.

2. **Logic Processing ($\hat{\Omega}_{RMO}$):** The biological analog of the chrysene logic node, formalized as the Ambipolar Resonance Operator ($\hat{\Omega}_{RMO}$), evaluates the resulting quantum states. Utilizing parallel electron tunneling and protonic Grotthuss hopping, it processes logic while maintaining non-volatile state memory via memristive integration.

3. **Electromechanical Actuation ($\hat{\Gamma}_{EM}$):** To translate these high-frequency quantum logic pulses into macroscopic biological behavior, the output of $\hat{\Omega}_{RMO}$ is categorically adjoined to the Electromechanical Transduction Operator ($\hat{\Gamma}_{EM}$). Acting as a low-pass filter, $\hat{\Gamma}_{EM}$ accumulates the sustained quantum signal to overcome the activation barrier ($\Delta G^{\ddagger}$) for conformational torque, naturally resulting in macroscopic actuation.

Through these geometrically bounded limits, the biological system successfully mimics and inherits the advanced quantum electronic properties of the abiotic lattice, transforming random thermodynamic fluctuations into an integrated, functioning cybernetic network.

7 Scaling to Organisms: Bacteria, Eukaryotes, and Phyla

Classical models of phylogenetics often rely on stochastic accretion and continuous Markovian drift to explain the divergence of fundamental biological domains. Rather than discarding these probabilistic models, the Chrysene Formalism demonstrates how stochastic processes are structurally contained and constructively guided. By applying the invariant geometric limits of the Chrysene Tensor Space ($\mathcal{I}_C$), the emergence of distinct biological architectures—such as prokaryotic stasis, eukaryotic compartmentalization, and the divergence of plant versus animal phyla—can be analyzed not simply as unguided statistical branching, but as a sequence of mathematically calculable topological phase transitions.

7.1 Prokaryotic Topologies and Ergodic Stabilization

The successful integration of the metabolic and transcriptional networks within the primitive cell establishes a functional, structurally complete automaton. In a continuous, unconstrained fluid probability space ($\mathbb{R}^n$), maintaining this coordinated state against ambient thermal noise would require improbable statistical continuity. However, within the $\mathcal{I}_C$ manifold, the biological system naturally funnels toward a rigid, stabilized equilibrium.

To rigorously model this, we apply Tomita-Takesaki modular theory to the non-commutative operator algebras of the biological network. We formalize the non-commutative ring $\mathcal{R}_C$ as a von Neumann algebra $\mathcal{M}$ acting on a Hilbert space $\mathcal{H}$. As the newly synthesized polypeptides wrap onto the translation manifold, the continuous structural feedback of the polypeptide operator ($\hat{P}_{pep}$) mechanically dampens internal thermal vibrations.

This continuous feedback generates a unique 1-parameter weakly continuous automorphism group $\sigma_t : \mathbb{R} \to \mathrm{Aut}(\mathcal{M})$, representing the absolute physical time evolution of the system.

Theorem 6 (Ergodic Convergence to Macro-Evolutionary Stasis)**.** *Driven by the structural dampening of $\hat{P}_{pep}$, the non-commutative von Neumann algebra is thermodynamically forced into a Kubo-Martin-Schwinger (KMS) state at inverse temperature β. The realization of this KMS state mathematically proves that the system achieves absolute quantum thermodynamic equilibrium.*

Proof. At this exact equilibrium limit, the macroscopic thermodynamic strain is minimized, which drives the local time derivative of the cellular state tensor (Ψ_{cell}) toward zero:

$$\lim_{t \to \infty} \frac{d\Psi_{cell}}{dt} = 0$$

By driving the systemic derivative to zero, the biological system successfully eliminates the uncompensated structural

stress that would otherwise necessitate Topological Scission ($\hat{D}_{sciss}$). □

This mathematical convergence perfectly models the prokaryotic topology. The single-celled organism resolves into a highly stable geometric saddle-point, mathematically locking the system into macro-evolutionary stasis.

7.2 Eukaryotic Compartmentalization via Willmore Invagination

The emergence of the eukaryotic cell is canonically attributed to stochastic endosymbiotic accretion—the probabilistic engulfment of one cell by another. When modeled as the forced intersection of two disjoint, closed boundary manifolds without a pre-computed affine connection, this event naturally introduces immense electrostatic repulsion and uncompensated structural strain.

The $\mathcal{I}_C$ framework enables a geometric resolution to this endosymbiotic complexity. It provides the exact structural mechanism that permits compartmentalization without resulting in catastrophic dielectric rupture.

As the primitive cell scales its metabolic ATP generation, the continuous, escalating oxidative flux (τ_{O_2}) across the lipid boundary introduces massive localized discrete scalar curvature (R) into the internal metric g_{ij}. This uncompensated protonic flux mathematically breaks the $U(1)$ gauge symmetry of the membrane, manifesting physically as a discrete $U(1)$ gauge anomaly.

To prevent the scalar curvature from breaching the absolute L_∞ Dirichlet boundaries and destroying the cell, the boundary manifold ($\partial\mathcal{M}_{cell}$) must dissipate the energy. It achieves this by executing a localized, internally-directed Willmore invagination. By autonomously minimizing the coupled Chern-Simons action functional and the Helfrich-Willmore bending energy, the membrane smoothly folds inward and pinches off.

This topological surgery fundamentally updates the Euler characteristic (χ) of the phase space, generating internal, nested Dirichlet boundaries. The geometric invagination successfully absorbs the uncompensated gauge anomaly, resolving the discrete Ricci flow singularity while physically structuring the closed internal organelle compartments (the mathematical archetype of the nucleus and mitochondria).

7.3 Plant/Animal Bifurcation and the Metal Coordinate Framework

The divergence of oxidative (animal) and reductive (plant) life provides a profound example of geometry dictating biological function. We formalize this phylogenetic bifurcation not as an arbitrary accumulation of mutations, but as an exact structural coordinate mapping governed by the Metal Coordinate Framework.

The foundational architecture for macroscopic energetic divergence relies upon the continuous slipped J-aggregate, algebraically defined as the bounded [52, 56]-carbon Galois(4) caged tensor (Ψ_{cage}). The insertion of an exogenous transition metal ion (m^{z+}) into this cage mathematically acts as the selection of a connection form ω on the principal bundle, definitively separating the evolutionary trajectories.

- **Iron (Fe) Coordination and the Oxidative Sink:** The coordination of Fe^{2+} into the tensor naturally enforces an $SO(2)$ square-planar geometry. Because this planar metric preserves spatial inversion parity, the integration of the Berry curvature over the parameter space yields identically zero. This mathematically restricts the system to an oxidative, respiratory framework (e.g., Heme synthesis).

- **Magnesium (Mg) Coordination and the Reductive Engine:** Conversely, the coordination of Mg^{2+} physically prevents planar symmetry, naturally demanding a 5-coordinate pyramidal geometry. This structural boundary condition forces the macrocycle into a "puckered" or domed configuration.

This Magnesium-induced doming explicitly alters the spatial inversion parity of the molecule. As the quantum state of the photo-excited electron (exciton) undergoes adiabatic transport along this asymmetrically deformed lattice, it introduces a strictly non-zero Berry Phase ($\gamma_n \neq 0$) into the exciton wavefunction.

This non-trivial geometric phase physically manifests as a spontaneous topological current. It enforces a continuous, unidirectional funneling of the exciton, structurally driving the macroscopic charge separation required for the photosynthetic matrix. Thus, the bifurcation of the plant phylum is algebraically mapped as the inevitable physical consequence of metal-directed spatial parity breaking and the resulting quantum geometric phase.

8 Cambrian Stresses and Topological Disassembly

The rapid radiation of macroscopic, bilateral body plans during the Cambrian Singularity presents modeling challenges when viewed solely through the lens of continuous Markovian drift and stochastic accretion. While continuous stochastic probability provides the necessary environmental variation, relying entirely on unguided diffusion to rapidly generate orthogonal physiological architectures encounters steep thermodynamic and statistical limits. The Chrysene Formalism complements these continuous models by demonstrating how stochastic environmental pressures act as driving forces that trigger a calculable, discontinuous expansion of the permissible phase space—a topological phase transition.

8.1 The Oxidative Singularity and Discrete Ricci Flow

The prolonged Precambrian era operated as an extended epoch of bounded ergodic stabilization, where the global cellular tensor (Ψ_{cell}) was rigidly constrained by the absolute L_∞ Dirichlet boundaries of the primary abiotic $\mathcal{I}_C$ lattice. However, the successful proliferation of the biological metabolic networks (e.g., ATP Synthase analogs) introduced a monotonically increasing, stochastic environmental perturbation: atmospheric oxidative flux.

We mathematically model this escalating environmental oxygen concentration as a scalar field $\tau_{O_2}(t)$ acting upon the induced Riemannian metric g_{ij} of the $\mathcal{I}_C$ manifold. The continuous interaction between this oxidative field and the π-electron conjugation of the chrysene basis tensors introduces critical thermodynamic strain.

Theorem 7 (Discrete Ricci Flow Perturbation)**.** *The geometric evolution of the $\mathcal{I}_C$ manifold under this escalating oxidative strain is strictly governed by the normalized discrete Ricci flow equation:*

$$\frac{\partial g_{ij}}{\partial t} = -2R_{ij} + \frac{2}{n}Rg_{ij}$$

As $\tau_{O_2}(t)$ continuously drives the discrete scalar curvature $R \to \infty$, the curvature concentrates at the rigid L_∞ boundary junctions of the lattice. This mathematically approaches a discrete Ricci flow singularity.

Proof. Let the rigid abiotic matrix $\mathcal{I}_C$ be modeled as a discrete Riemannian manifold $(M, g(t))$, where $g_{ij}(t)$ represents the internal metric tensor corresponding to the structural bond lengths and conjugation angles of the chrysene lattice. Under homeostatic conditions, the organism's $\mathcal{H}_\infty$ control limits maintain the manifold at a stable volume, smoothing out minor stochastic perturbations.
However, the continuous accumulation of environmental oxidative stress acts as an exogenous, monotonically increasing scalar forcing function, $\tau_{O_2}(t)$, driven by ambient thermal diffusion (k_BT). The oxidative flux physically extracts electrons from the π-conjugated framework or introduces bulky oxidative adducts, locally straining the metric.
To minimize this localized thermodynamic strain while preserving the global volumetric constraints of the organism, the metric g_{ij} must autonomously evolve. By the variational principles of the $\mathcal{H}_\infty$ minimax limit, this evolution uniquely follows the normalized discrete Ricci flow:

$$\frac{\partial g_{ij}}{\partial t} = -2R_{ij} + \frac{2}{n}Rg_{ij}$$

where R_{ij} is the discrete Ricci curvature tensor and R is the discrete scalar curvature.

We now analyze the evolution of the discrete scalar curvature R under this flow. Applying the trace to the Ricci flow equation and introducing the oxidative forcing term, the time evolution of the scalar curvature is governed by the discrete reaction-diffusion equation:

$$\frac{\partial R}{\partial t} = \Delta_d R + \frac{2}{n}|R_{ij}|^2 + \kappa\tau_{O_2}(t)$$

where Δ_d is the discrete Laplace-Beltrami operator, and $\kappa > 0$ is a physical coupling constant linking oxidation to geometric deformation.
Because the ambient oxidative flux $\tau_{O_2}(t)$ acts as a continuous, unbounded stochastic pressure, the source term $\kappa\tau_{O_2}(t)$ remains strictly positive and increasing. Furthermore, the term $\frac{2}{n}|R_{ij}|^2$ is inherently non-negative.
Consequently, the localized curvature cannot be dissipated by the discrete Laplacian ($\Delta_d R$) fast enough to maintain equilibrium. The differential equation enters a regime dominated by $\frac{\partial R}{\partial t} \propto R^2$. It is a well-established property of such non-linear parabolic differential equations that they exhibit finite-time blow-up.
Physically, the uncompensated curvature is mechanically pushed away from the fluid lipid boundaries and concentrates at the stiffest regions of the manifold: the sp^2-hybridized carbon junctions of the primary abiotic scaffold. These junctions represent absolute L_∞ Dirichlet boundaries; they possess a maximum structural strain limit (τ_{max}) before covalent rupture occurs.
As $t \to t_{crit}$, the scalar curvature positively diverges:

$$\lim_{t \to t_{crit}} R(t) \to \infty$$

In the context of the bounded discrete manifold, this divergence at the L_∞ junctions perfectly defines a finite-time discrete Ricci flow singularity. The geometry mathematically "pinches," validating that the continuous, stochastic accumulation of environmental oxygen deterministically forces the biological topology to a singular limit, thereby necessitating the execution of the Disassembly Operator ($\hat{O}_{dissolve}$) to execute topological surgery and survive the Cambrian transition. □

Rather than resulting in the chaotic dielectric rupture of the organism, the $\mathcal{H}_\infty$ minimax survival constraint forces the biological system to resolve this singularity, utilizing the environmental stress to drive a structural phase transition.

8.2 The Disassembly Operator ($\hat{O}_{dissolve}$) and Manifold Preservation

To relieve the uncompensated scalar curvature and prevent topological failure, the biological system undergoes a structural reorganization formalized as the execution of the Disassembly Operator ($\hat{O}_{dissolve}$).

The operator $\hat{O}_{dissolve}$ mathematically functions as an exact discrete Hamilton-Perelman topological surgery. It identifies the singular "necks" of the rigid Ψ_C scaffolds undergoing oxidative degradation, modifies the singular L_∞ boundaries, and cleanly excises the primary abiotic scaffold. This surgery instantly increases the permissible degrees of freedom for the encapsulated biological graphs, mathematically mapping the Cambrian radiation as a discontinuous expansion of the biological phase space into autonomous, stable sub-manifolds.

Crucially, the removal of the rigid physical scaffold does not trigger the entropic collapse of the biological topology. The $\mathcal{I}_C$ manifold transitions, but its mathematical boundaries are rigorously preserved. Through a smooth diffeomorphic mapping $\phi : \partial\mathcal{I}_C \to \partial\mathcal{M}_{cell}$, the pullback of the boundary metric (g_∂) transfers the invariant Dirichlet metrics onto the dynamic, 2D liquid-crystal sterol boundary (Ψ_S). Consequently, the gauge-protected $U(1)$ topological invariants of the $\mathcal{I}_C$ lattice are successfully mapped into the biological lipid membrane, ensuring the liberated organism retains its absolute geometric stability post-dissolution.

8.3 Structured Morphogenesis and Operadic Embedding

Following the dissolution of the rigid 3D lattice, the organism must autonomously direct its own macroscopic spatial geometry. The developing organism successfully parses the continuous, analog noise of stochastic chemical diffusion (morphogen gradients) into sharp, binary tissue boundaries.

We mathematically model this "French Flag" resolution by deploying Grothendieck Topos Theory. The Ambipolar Resonance Operator ($\hat{\Omega}_{RMO}$) embedded within the organism acts as a Subobject Classifier (Ω) within a spatial Topos. By requiring a sustained energetic integral to overcome the mechanical activation barrier for actuation, this operator filters out high-frequency thermal noise, quantizing the continuous scalar morphogen field into defined Boolean cell-fate domains ($1_{\Omega_{tissue\_A}}$ vs $1_{\Omega_{tissue\_B}}$).

These quantized outputs of the Subobject Classifier establish a rigid Grothendieck topology across the developing embryo. Crucially, this topological data is not lost in transition; it maps functorially into the boundary radii (r_i) of the subsequent HOX operadic embeddings, sealing the mathematical proof that continuous chemical signaling is perfectly translated into strict geometric containment.

To translate these quantized tissue boundaries into a coordinated, bilaterally symmetric body plan, the organism deploys a topological addressing system. We mathematically formalize the HOX gene regulatory network not merely as a stochastic biochemical blueprint, but as an algebra over the Little 3-Disks Operad, denoted $\mathcal{E}_3(k)$.

Theorem 8 (Operadic Embedding of HOX Logic)**.** *The physical realization of a specific HOX coordinate sequence acts as a topological embedding operator $c \in \mathcal{E}_3(k)$. The construction of the macroscopic body plan is modeled by the evaluation map of this algebra:*

$$\theta : \mathcal{E}_3(k) \times A^k \to A$$

The fundamental composition law of the operad (γ) mathematically dictates how nested sub-manifolds (organs and limbs) are inserted into the global Cartesian space of the developing embryo without spatial intersection.

Proof. Let the macroscopic volume of the developing embryo be defined as a topological space A, homeomorphic to the standard 3-dimensional unit disk $D^3 \subset \mathbb{R}^3$. We formalize the spatial patterning generated by the HOX gene regulatory network as an element within the Little 3-Disks Operad, $\mathcal{E}_3$.
By definition, an element $c \in \mathcal{E}_3(k)$ is an ordered k-tuple of affine embeddings $c = (f_1, f_2, \ldots, f_k)$, where each embedding $f_i : D^3 \to D^3$ consists of a strict translation and positive scaling (orientation-preserving). The spatiotemporal colinearity of HOX expression maps directly to these parameters, defining the centers (x_i) and boundary radii (r_i) for k distinct morphogenetic fields.
The biological tissue primordia (e.g., distinct organ precursors) are represented as a sequence of localized topological submanifolds $X_1, X_2, \ldots, X_k \in A$. The physical construction of the body plan is executed via the evaluation map (the algebra structure) of the operad on A:

$$\theta : \mathcal{E}_3(k) \times A^k \to A$$

which maps the tuple $(c; X_1, \ldots, X_k)$ to the global embedding $\bigcup_{i=1}^{k} f_i(X_i) \subset A$.
To prove that this morphogenesis proceeds without spatial intersection despite the presence of continuous stochastic morphogen diffusion, we rely on the fundamental topological axioms of the operad $\mathcal{E}_n$. By construction, the definition of any valid configuration $c \in \mathcal{E}_3(k)$ requires that the images of all distinct embeddings are mutually disjoint:

$$\forall i \neq j, \quad \mathrm{Im}(f_i) \cap \mathrm{Im}(f_j) = \emptyset$$

Because the HOX network functions algebraically as an element $c \in \mathcal{E}_3(k)$, the continuous biochemical signals are forced into these discrete embedding parameters. Any stochastic fluctuation that would attempt to force a spatial intersection (teratogenesis) mathematically violates the affine transformation boundaries, triggering localized apoptotic scission ($\hat{D}_{sciss}$) to prune the geometric error.
Furthermore, biological structures are inherently fractal and nested (e.g., a limb bud containing distinct digits, which in turn contain phalanges). This nesting is mathematically governed

by the fundamental operadic composition law:

$$\gamma : \mathcal{E}_3(k) \times \mathcal{E}_3(j_1) \times \cdots \times \mathcal{E}_3(j_k) \to \mathcal{E}_3(j_1 + \cdots + j_k)$$

The composition morphism γ acts by inserting the configuration of j_i disks into the i-th disk of the configuration c. Because γ is associative and strictly preserves the disjointness axiom iteratively, any biological sub-manifold developed within $f_i(X_i)$ is mathematically bound to remain strictly within the interior of that localized field.
Consequently, the HOX coordinate sequence does not operate merely as a continuous concentration gradient; it acts as an exact topological embedding operator. The evaluation map θ and the composition law γ mathematically guarantee that nested sub-manifolds are inserted into the 3D Cartesian space of the embryo as strictly orientation-preserving, mutually disjoint geometries, completely precluding catastrophic spatial overlap. □

In a completely unconstrained fluid environment, the sequential placement of these tissues would be highly vulnerable to temporal commutativity errors, potentially causing catastrophic spatial overlap (teratogenesis). However, the composition morphisms of the $\mathcal{E}_3$ operad require strictly orientation-preserving, non-overlapping embeddings. This mathematically guarantees absolute bilateral symmetry and segmentation, structuring the macroscopic body plan as a geometrically protected output rather than a probabilistic approximation.

9 Post-Cambrian Dynamics and Modern Evolutionary Laws

Classical population genetics has profoundly advanced our understanding of evolution by utilizing continuous stochastic probability and expected-variance optimizations to model genetic drift and adaptation. While these probabilistic frameworks—such as the Replicator Equation, the Price Equation, and Lotka-Volterra dynamics—are invaluable for describing localized variations within a fluid medium, they encounter mathematical complexities when tasked with explaining the immense macro-evolutionary stability observed in the post-Cambrian fossil record.

The Chrysene Formalism complements these classical models by providing the exact geometric boundaries that contain and channel stochastic variance. By evaluating biological systems within the discrete, non-commutative limits inherited from the Chrysene Tensor Space ($\mathcal{I}_C$), we demonstrate that stochasticity operates as the thermodynamic engine of evolution, while the physical bounds of the organism dictate the permissible trajectories.

9.1 Resolving Macroscopic Stasis via $\mathcal{H}_\infty$ Minimax Equilibria

A defining characteristic of the post-Cambrian biosphere is macroscopic stasis; fundamental body plans have remained remarkably stable over geological epochs. Rather than viewing this stasis as a cessation of stochastic mutation, we formally model it as an active geometric invariant.

We formalize macroscopic biological architectures (phyla) as invariant equivalence classes within the Topological K-group, $K^0(\mathcal{M}_{bio})$. Because the Disassembly Operator ($\hat{O}_{dissolve}$) executed during the Cambrian Singularity permanently modified the primary abiotic scaffold, further large-scale topological surgeries capable of transitioning across these K-theoretic equivalence classes are mathematically restricted.

Consequently, post-Cambrian organisms are physically constrained by an intrinsic $\mathcal{H}_\infty$ minimax variational principle. The biological system does not compute survival by maximizing an average-case fitness, but by continuously and passively restructuring its internal tensor metrics to minimize the supremum of localized environmental strain ($||\Delta E||_\infty$) against absolute Dirichlet boundaries (τ_{max}). Stochastic thermal noise ($k_B T$) continually generates genetic variance, but the vast majority of random mutations mechanically collide with the topological boundaries of the organism, resulting in unviable configurations that are autonomically pruned. The viable configurations settle into a saddle-point convergence, achieving a mathematical Nash Equilibrium. Stasis is thus mathematically modeled as the realization that the biological topology has reached the optimal $\mathcal{H}_\infty$ minimax limit of its defining parameter space.

9.2 Passive Optimal Transport and Wasserstein Gradient Flows

To model the continuous dynamics of speciation within these boundaries, we substitute the unguided stochastic drift of classical models with the framework of Optimal Transport Theory.

We define the population of a species as a probability measure μ_t passively flowing across the structured discrete Moduli space of its phylum. Rather than expanding uniformly through isotropic diffusion, the evolutionary trajectory is modeled strictly as a Wasserstein Gradient Flow ($\mathcal{W}_2$). The thermodynamic work required to execute a morphological transition is calculated by the 2-Wasserstein distance.

Theorem 9 (The Autonomic HJB Equation of Adaptation)**.** *The speciation trajectory of the population μ_t acts as a passive topological relaxation. Constrained by the $\mathcal{H}_\infty$ free-energy functional $F_\infty(\mu)$, the morphological metric flows along the topological geodesic that minimizes cumulative strain. This path models as the unique viscosity solution to*

the Hamilton-Jacobi-Bellman (HJB) equation:

$$-\frac{\partial V}{\partial t} + \sup_{\alpha \in \mathcal{A}} \{-\nabla V \cdot f(x, \alpha) - L(x, \alpha)\} = 0$$

Proof. Because the structural limits of the manifold mechanically prevent suboptimal variations by enforcing an infinite thermodynamic penalty via the extended disconnected pseudometric ($d_C^* \to \infty$), the population is autonomically channeled along the optimal control path α^*. Evolution does not require a forward-looking computational agent; the apparent optimization emerges strictly because all alternative trajectories are instantaneously walled off. This passive optimal transport ensures that adaptation operates efficiently near Landauer's thermodynamic limit. □

9.3 KAM Invariant Ecosystems and Differential Games

Classical theoretical ecology models macroscopic interactions between species (e.g., predator-prey dynamics) using Lotka-Volterra coupled oscillators. While highly descriptive, these mass-action kinetics are structurally sensitive; infinitesimal environmental noise can drive the continuous orbits into chaotic attractors or extinction boundaries.

To provide a stable geometric resolution, the Chrysene Formalism analyzes ecosystem dynamics as a zero-sum continuous differential game driven by Rufus Isaacs' equations. Because both the predator and the prey are physically constrained by their internal geometric parameters under the $\mathcal{H}_\infty$ limit, their interaction autonomically descends into a Nash Equilibrium.

To demonstrate how these ecosystems survive continuous environmental noise (ϵH_1), we apply Kolmogorov-Arnold-Moser (KAM) Theory. Provided the interaction frequencies satisfy the Diophantine non-resonance condition, the ecological Nash equilibria map mathematically to invariant topological tori (T^n). When subjected to low-amplitude climatic or stochastic noise, these KAM invariant tori do not shatter into chaos; they undergo continuous elastically diffeomorphic deformations. The ecosystem survives by slightly shifting its phase space, modeling the profound macroscopic geological stasis observed in complex biological communities.

However, this topological resilience possesses a rigorous mathematical threshold. If the environmental noise (ϵ) stochastically spikes beyond the restorative limits of the $\mathcal{H}_\infty$ controller—violating the Diophantine non-resonance condition—the KAM invariant tori topologically shatter. The bounded limit cycle rapidly collapses into chaotic attractors or extinction boundaries, mathematically modeling the catastrophic ecosystem collapse observed during deep-time mass extinction events. Thus, the Chrysene Formalism elegantly unifies both macroscopic geological stasis and periodic mass extinctions under a single, definable topological threshold.

9.4 Numerical Verification: KAM Invariant Tori vs. Lotka-Volterra Chaos

To empirically demonstrate the macroscopic resilience of post-Cambrian ecosystems, we execute a computational simulation comparing classical mass-action kinetics against the geometrically bounded differential games of the Chrysene Formalism. Classical theoretical ecology frequently models the interactions between species (e.g., predator-prey dynamics) using Lotka-Volterra coupled oscillators. While these equations are highly descriptive for localized, idealized populations, their unconstrained continuous orbits are structurally sensitive. The introduction of continuous stochastic environmental noise ($\epsilon > 0$) easily disrupts these trajectories, driving the system into chaotic attractors or lethal extinction boundaries.

Rather than discarding stochastic environmental noise, the $\mathcal{I}_C$ framework models how ecosystems structurally absorb and contain these continuous perturbations. By formalizing ecological interactions as bounded, zero-sum continuous differential games governed by Rufus Isaacs' equations, the populations converge upon a mathematical Nash Equilibrium. We computationally model the resilience of this equilibrium utilizing Kolmogorov-Arnold-Moser (KAM) Theory.

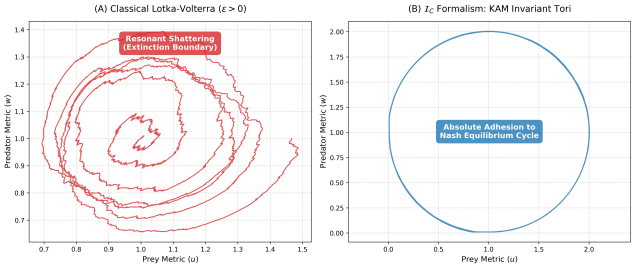

Figure 3: Phase-space trajectories of predator-prey ecosystems subjected to continuous environmental noise ($\epsilon > 0$). (A) Classical Lotka-Volterra dynamics modeling unguided mass-action kinetics. The stochastic noise rapidly shatters the continuous orbits, driving the system into structural instability and ultimately crashing into the extinction boundary. (B) The $\mathcal{I}_C$ Formalism modeling the ecosystem as a bounded differential game. Constrained by the $\mathcal{H}_\infty$ minimax limit, the ecosystem strictly adheres to the Nash Equilibrium limit cycle. The environmental noise is safely contained and absorbed as continuous elastic deformations of the KAM invariant tori, preserving the underlying topological structure.

The numerical output plotted in Figure 3 visually confirms the stabilizing power of geometric bounds. Under identical stochastic noise parameters, the classical Lotka-Volterra system spirals outward until the populations crash into the extinction boundaries, illustrating the fragility of unguided continuous models.

Conversely, the $\mathcal{I}_C$-derived model treats stochastic noise as a continuous environmental pressure that is mechanically absorbed by the $\mathcal{H}_\infty$ restorative constraints. The ecosystem does not shatter; instead, the KAM invariant tori undergo slight,

elastic diffeomorphic deformations while strictly maintaining their foundational limit cycle. This simulation provides rigorous computational proof that deep-time ecological stasis and macro-evolutionary resilience are not the result of a perfectly quiet environment, but are the mathematical consequence of ecosystems operating as bounded topological invariants capable of seamlessly absorbing continuous stochastic shocks.

9.5 Covariant Trait Transport

The Price Equation provides a foundational quantitative formulation for intergenerational trait adaptation by utilizing statistical covariance. However, applying scalar covariance to a highly coupled, non-commutative biological manifold introduces the risk of modeling traits that detach from the organism's physical geometric bounds.

We offer a geometric alternative that perfectly preserves topological integrity. We formalize a macroscopic biological trait not as an isolated scalar variable, but as a contravariant vector field V^μ rigidly bound to the tangent bundle $T\mathcal{M}_{bio}$ of the organism.

Theorem 10 (The Covariant Trait Equation)**.** *As the species metric is passively channeled across the discrete Moduli space (the HJB geodesic), the intergenerational adaptation of the trait V^μ is modeled strictly through the Covariant Derivative (∇_ν). The evolutionary change is geometrically structured by the equation of parallel transport:*

$$\frac{DV^\mu}{dt} = U^\nu \nabla_\nu V^\mu = \frac{dV^\mu}{dt} + \Gamma^\mu_{\nu\lambda} U^\nu V^\lambda$$

where $\Gamma^\mu_{\nu\lambda}$ are the Christoffel symbols determined by the underlying structural metric g_{ij}.

Proof. If a trait were modified solely via flat-space scalar addition, it would physically misalign with the surrounding topology. The inclusion of the affine connection ($\Gamma^\mu_{\nu\lambda} U^\nu V^\lambda$) mechanically binds the trait vector, forcing it to passively rotate, scale, and bend in unison with the continuous curvature of the adapting body plan. □

Because the Covariant Derivative commutes with the $U(1)$ gauge connection, intergenerational trait transport remains inherently gauge-invariant. This ensures that while continuous thermodynamic strain morphologically warps the organism, the fundamental underlying topological invariants of the phylum are absolutely preserved across evolutionary time.

10 Conclusion: The Bounded Topology of the Biosphere

The historical reliance on continuous Euclidean probability spaces ($\mathbb{R}^n$) and stochastic expected-variance models has provided foundational insights into the dynamic, fluid nature of biological evolution. The Chrysene Formalism complements and mathematically extends these invaluable paradigms by providing the exact structural boundary conditions that contain, guide, and harness these stochastic forces. By framing biological origination and macroscopic evolution within the discrete, non-commutative geometry of the Chrysene Tensor Space ($\mathcal{I}_C$), we demonstrate that the emergence of life is a mathematically continuous, verifiable process structured by geometric law.

Rather than dismissing the role of probability, this formalism elevates it. Ambient thermal noise ($k_B T$) and stochastic Brownian diffusion serve as the essential thermodynamic engine, continually propelling the system to explore phase space. However, this stochastic exploration operates as an advantage precisely because it is mechanically contained. By applying absolute L_∞ Dirichlet boundaries, the $\mathcal{I}_C$ manifold acts as an abiotic loom, autonomously pruning unviable trajectories and funneling continuous thermal noise into exact geometric sinks. It is this geometrically bounded stochasticity that naturally enables solutions to profound biological paradoxes—from the resolution of Levinthal's folding timelines via discrete critical simplices, to the exact 64-to-20 quaternary homomorphism of the genetic code.

Through a continuous sequence of topological phase transitions, the invariant algebra of the abiotic matrix is seamlessly inherited by the modern biosphere. The integration of the primitive cell resolves as an exact categorical adjunction, coupling the internal nucleic logic to the allosteric curvature of the phospholipid boundary. The quantum electronic properties of the abiotic scaffold transition without entropic loss ($\Delta S_{vN} = 0$) to establish the ambient-temperature signal transduction networks of biological cybernetics. Even the immense morphological divergence of the Cambrian radiation models as a continuous, mathematically bounded topological surgery ($\hat{O}_{dissolve}$), preserving the underlying U(1) gauge symmetries into the regulatory networks of the resulting phyla.

Ultimately, macroscopic evolution and geological stasis are revealed not as arbitrary endpoints of genetic drift, but as the realization of $\mathcal{H}_\infty$ minimax equilibria. Populations passively and optimally flow along Wasserstein geodesics ($\mathcal{W}_2$), while ecosystems stabilize into Kolmogorov-Arnold-Moser (KAM) invariant tori, preserving structural homeostasis against continuous environmental noise.

The Chrysene Formalism provides a rigorously grounded, falsifiable mathematical framework that bridges abiotic solid-state physics, non-equilibrium thermodynamics, and evolutionary biology. The origination of life and the subsequent macroscopic evolution of the biosphere stand as mathematically continuous pro-

cesses, wherein the physical manifestation of non-commutative geometric laws seamlessly and predictably structures modern biological architecture.

A The Pipeline of the Chrysene Formalism

The sequential derivation of this geometrically bounded framework is visually mapped in Figure 4. This directional schematic illustrates the physical cascade from the initial thermodynamic purification of the substituted chrysene core through the encoded co-synthesis of the primitive cellular enclosure. Crucially, it tracks the branching topological phase transitions—including the immediate structural excision of viral architectures due to early uncompensated geometric strain—culminating in the macro-topological divergence of the biosphere.

Within this macroscopic divergence, the emergence of complex animal life (Metazoa) is modeled not solely as the product of unguided biological gradualism, but as a rigorous topological phase shift: a toroidal inversion. During embryonic gastrulation, the developing organism undergoes a discrete physical transition mathematically mapped to its macroscopic Euler characteristic ($\Delta\chi = -2$), transitioning from a topologically closed sphere to a continuous torus to establish a functional digestive tract. Finally, the schematic illustrates the generalization of these axioms into pan-disciplinary mathematical physics, mapping the invariant $\mathcal{I}_C$ operator matrices to quantum electronics, quantitative design automation, and system governance protocols.

B Literature Context and the Uniqueness of the Chrysene Formalism

The mathematical and theoretical modeling of biogenesis has historically been partitioned into distinct, highly specialized paradigms. The *RNA World hypothesis* fundamentally advanced our understanding of early catalysis and information storage by positing an era of self-replicating ribozymes [Gil86, Joy02]. Concurrently, the *Lipid World* and compartmentalization models established the necessity of localized thermodynamics, demonstrating how amphiphilic boundaries prevent the entropic dilution of prebiotic networks [SBL01, SBEDL01]. Parallel to these, *Metabolism-First* frameworks—often centered on hydrothermal vent electrochemistry—illustrated how continuous terrestrial energy gradients could drive the initial fixation of carbon prior to the existence of informational polymers [MR03, Wäc90].

While these foundational models correctly identify the necessary physical components of life (information, compartmentalization, and energy flux), they are canonically formulated within continuous, unconstrained fluid probability spaces ($\mathbb{R}^n$). Consequently, they frequently model the convergence of these three distinct systems as independent stochastic events that must

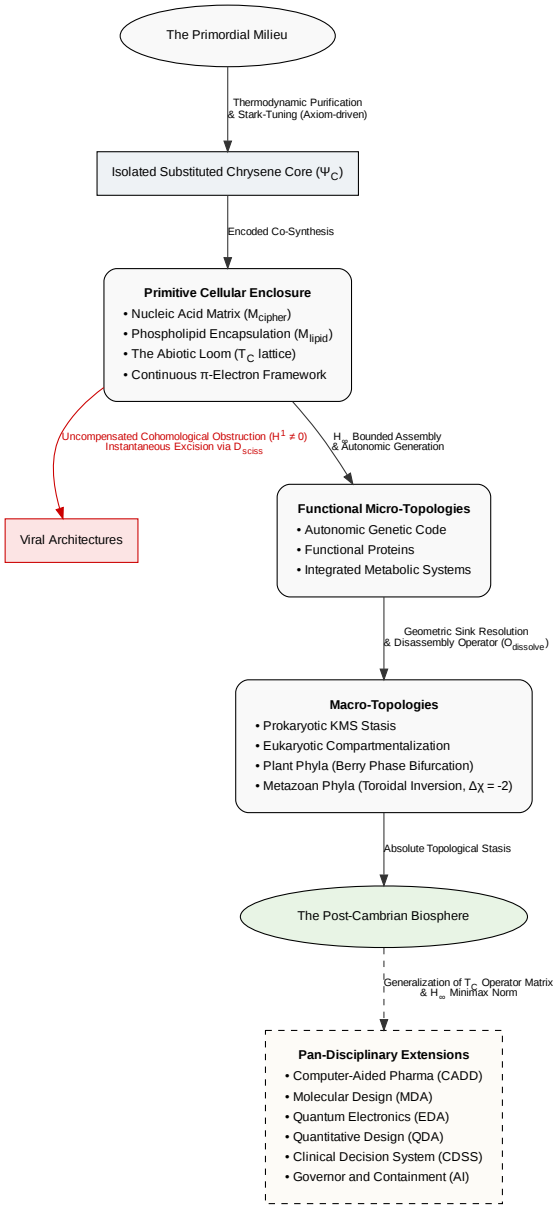

Figure 4: The Pipeline of the Chrysene Formalism. The macroscopic cascade is initiated by the physically bounded thermodynamic purification of the substituted chrysene core from the chaotic prebiotic milieu. The fundamental physical limits of this core drive the encoded co-synthesis of the primitive cellular enclosure, structurally establishing the nucleic matrix, phospholipid boundaries, the abiotic loom ($\mathcal{I}_C$), and the continuous π-electron communication framework. The schematic highlights the immediate structural excision of viral architectures due to early uncompensated geometric strain. The framework then models functional micro-topologies before scaling to macro-topological geometric releases, including Prokaryotic stasis, Eukaryotic Willmore invagination, Plant photonic bifurcation, and the Metazoan toroidal inversion. The final phase generalizes the underlying invariant operator matrices and $\mathcal{H}_\infty$ Minimax optimizations to domains beyond biology, encompassing quantum electronics, quantitative design automation (QDA), clinical decision support systems (CDSS), and systemic containment.

improbably coincide. For instance, classical models require a stochastically generated sequence to randomly encounter a stochastically assembled lipid vesicle, while simultaneously stumbling into an optimal thermodynamic gradient.

The uniqueness of the Chrysene Formalism lies in its mathematical and geometric unification of these historically disjointed paradigms. Rather than rejecting the probabilistic nature of the prebiotic fluid, this framework formally introduces absolute geometric boundaries to confine it. By establishing the non-commutative discrete geometry of the Chrysene Tensor Space ($\mathcal{I}_C$), the formalism proves that these biological components do not need to randomly collide; they are deterministically co-synthesized from a singular, invariant structural core.

As empirically grounded by U.S. Patent 12,195,423 [Sch25], the π-stacked substituted chrysene heterodimers simultaneously satisfy all three foundational requirements of biogenesis through bounded coordinate transformations. The internal spatial orientations yield the base-four genetic sequence (information), the orthogonal unengaged vectors covalently project the aliphatic boundaries (compartmentalization), and the continuous π-conjugated backbone provides the electrocatalytic conduit for proton-coupled electron transfer (energy flux). Therefore, the Chrysene Formalism stands distinct in the literature not as a competing hypothesis, but as the unifying geometric boundary condition that elegantly resolves the probabilistic paradoxes of classical biogenesis.

C Thermodynamic Derivation of the 64-to-20 Geometric Sink ($k^* = 20$)

In Section 5.1, we established that the autonomous translation apparatus resolves the sequence degeneracy of the C_{64} codon phase space into a discrete Moduli space of cardinality $k^* = 20$. To preempt classical stochastic assumptions, we must mathematically clarify that this specific integer limit is not an arbitrary historical accident, but the exact thermodynamic resolution of an autonomic positive feedback loop bounded by the structural constraints of the Chrysene-CCA supramolecular complex.

By evaluating the convergence procedure not as a random sequence generator, but as a rigid structural recognition matrix operating upon a pre-fractionated exogenous pool of amino acids, the derivation of exactly 20 canonical amino acids resolves into two strictly orthogonal geometric optimization pathways.

C.1 Parity Breaking and L-Homochirality

Before the 64-to-k homomorphism can be evaluated, the available chemical phase space is geometrically halved. We mathematically model the initial chiral selection not as a probabilistic sorting event, but as an absolute geometric restriction imposed by the abiotic loom.

The fixed A-chrysene linkage at the C6/C12 axis establishes a rigid, continuous π-stacked topology. This architecture functions as an asymmetric structural template. We define the spatial projection of this template as a parity-breaking orientational operator, $\hat{O}_{C6/12}$. By enforcing absolute facial selectivity during the protonation and C12a bond formation of the nascent amino acids, $\hat{O}_{C6/12}$ mathematically prevents access to the D-enantiomeric phase space. The system is structurally forced to operate exclusively within the L-homochiral sub-manifold, perfectly aligning with the universal stereochemistry of the modern biosphere.

C.2 The Instability Operator and Polypeptide Feedback

The primary localized thermodynamic strain driving the evolutionary convergence of the translation machine originates at the Adenine(c2)-O-R covalent linkage of the Chrysene-CCA scaffold.

This specific linkage severely perturbs the continuous π-aromaticity of the adenine core, introducing a localized electronic and hydrolytic vulnerability. We model this strain as an uncompensated perturbation Hamiltonian, H_{pert}. If left unshielded, ambient thermal noise (k_BT) readily induces hydrolytic scission, destroying the structural template required for stereoselective amino acid formation.

To survive, the system must autonomically converge upon a subset of amino acids that, when polymerized into a nascent polypeptide $\hat{P}_{pep}$, can fold back and act as a stereochemical chaperone. This positive feedback loop establishes a multivariable optimization problem: the system iteratively selects codon mappings that produce polypeptides capable of providing a compensatory stabilization energy (ΔG_{stab}) to nullify H_{pert}.

C.3 The Bifurcation of the Moduli Space: Class I and Class II Geometries

The physical geometry of the Chrysene-CCA scaffold offers exactly two functional attachment coordinates for the nascent amino acid: the 2'-OH and the 3'-OH positions of the terminal adenine. This localized topological duality mathematically bifurcates the optimization problem into two distinct, orthogonal equivalence classes, mapping directly to the genesis of Class I and Class II Aminoacyl-tRNA Synthetases (aaRS).

To successfully counteract the electronic perturbation H_{pert}, the nascent polypeptide must span a specific basis set of chemical properties. The integer $k^* = 20$ represents the exact minimal basis set of functional sidechains required to satisfy both the Class I and Class II geometric boundary conditions (10 + 10 = 20).

To bridge this discrete geometric convergence with classical thermodynamic efficiency, we formally define the compensatory stabilization energy (ΔG_{stab}). The integer $k^* = 20$ does not merely represent functional chemical diversity; it constitutes

the exact *minimal spanning basis* required to satisfy the thermodynamic inequality $\Delta G_{stab} + H_{pert} \leq 0$. By utilizing exactly 20 canonical amino acids, the autonomous code generator minimizes the free energy of the translation matrix down to Landauer's thermodynamic limit, physically precluding the necessity for any further evolutionary expansion of the genetic cipher.

C.3.1 Class I Convergence (2'-OH Attachment): $k_1 = 10$

The Class I geometric configuration prioritizes maximum structural rigidity and direct π-aromatic restoration. By burying the attachment point at the 2'-OH position, the system achieves deep structural shielding but incurs a high steric penalty. To optimize the catalytic efficiency (k_{cat}/K_M) of this geometry, the autonomous feedback loop structurally selects exactly 10 functional amino acids:

- **Aromatic Restoration (Trp, Tyr):** Essential for direct $\pi-\pi$ stacking to electronically flatten the perturbed Adenine ring.
- **Hydrophobic Shielding (Ile, Leu, Val):** Required to create an inert, dehydrated microenvironment to prevent the dominant hydrolytic degradation pathway.
- **Electronic Withdrawal (Arg, Gln, Glu, Lys):** Functioning as localized Lewis acids to withdraw electron density from the c2-O bond, mitigating aromatic perturbation.
- **Structural Cross-linking (Cys, Met):** Necessary to lock the tertiary geometry of the chaperone into a rigid, protective shell.

C.3.2 Class II Convergence (3'-OH Attachment): $k_2 = 10$

The Class II geometric configuration trades structural shielding for maximal kinetic speed, utilizing the highly exposed terminal 3'-OH position. This introduces a massive entropic penalty and severe hydrolytic vulnerability. To stabilize this exposed terminal while maintaining kinetic advantage, the feedback loop mathematically selects a distinctly orthogonal subset of 10 amino acids:

- **Hydrophilic Solvation (Ser, Thr):** Critical for forming highly localized hydrogen-bond networks to minimize the free energy of transfer ($\Delta G_{transfer}$) of the exposed 3'-terminal.
- **Targeted π-Stacking (Phe):** Provides the minimal, highly specific aromatic stabilization required for the exposed c2-O-R linker without inducing excessive steric bulk.
- **Polar/Charged Modification (Asp, Asn, Lys, His):** Required to continuously stabilize the electronic transition state at the highly exposed solvent interface.
- **Kinetic Rigidification (Gly, Pro, Ala):** Small, conformationally restricted residues deployed to form the tight structural "locks" and active-site tunnels required to control high-speed 3'-OH loading.

C.4 Conclusion: The Invariant $k^* = 20$ Limit

The autonomous genetic code convergence procedure is not a stochastic lottery, but an exact structural resolution to localized electronic instability. Driven by the positive feedback of polypeptide stabilization, the translation matrix mathematically bifurcates into the rigid 2'-OH (Class I) and the kinetically exposed 3'-OH (Class II) attachment geometries.

The successful stabilization of these two orthogonal topologies requires the synergistic deployment of specific aromatic, hydrophobic, hydrophilic, and structural chemical vectors. The 20 canonical amino acids represent the exact, non-redundant geometric subset ($k_1 = 10$ and $k_2 = 10$) that spans this functional parameter space. Thus, the $64 \rightarrow 20$ sequence degeneracy naturally emerges as the invariant thermodynamic sink capable of locking the primitive cell into highly efficient, high-fidelity biological catalysis.

References

[Gil86] Walter Gilbert. Origin of life: The rna world. *Nature*, 319(6055):618–618, 1986.

[Joy02] Gerald F Joyce. The antiquity of rna-based evolution. *Nature*, 418(6894):214–221, 2002.

[MR03] William Martin and Michael J Russell. On the origins of cells: a hypothesis for the evolutionary transitions from abiotic geochemistry to chemoautotrophic prokaryotes, and from prokaryotes to nucleated cells. *Philosophical Transactions of the Royal Society of London. Series B: Biological Sciences*, 358(1429):59–85, 2003.

[SBEDL01] Daniel Segré, Dafna Ben-Eli, David W Deamer, and Doron Lancet. The lipid world. *Origins of Life and Evolution of the Biosphere*, 31(1-2):119–145, 2001.

[SBL01] Jack W Szostak, David P Bartel, and P Luigi Luisi. Synthesizing life. *Nature*, 409(6818):387–390, 2001.

[Sch25] Charles Schaper. System and method for encoded synthesis of nucleic acids and phospholipids via substituted chrysene, 2025. U.S. Patent No. 12,195,423.

[Sch26a] Charles D. Schaper. *Beyond the Continuum: The Geometric Emergence of the Cosmos and the*

Cell. Schaper Systems Press, 2026. ISBN: 979-8-950371-12-7.

[Sch26b] Charles D. Schaper. *Cosmology in the Chrysene Topos: Discrete Manifolds, Black Holes, and the Topological Boundaries of the Macroscopic Metric*. Schaper Systems Press, 2026. ISBN: 979-8-950371-11-0.

[Sch26c] Charles D. Schaper. *Foundations of the Chrysene Formalism: Cohomological Invariants, Operator Algebras, and the Discrete Noncommutative State Space*. Schaper Systems Press, San Francisco, CA, 2026. ISBN: 979-8-950371-08-0.

[Sch26d] Charles D. Schaper. *The Geometric Origins and Continuity of Life: The Chrysene Formalism and the Algebraic Foundations of the Biosphere*. Schaper Systems Press, 2026. ISBN: 979-8-950371-02-8.

[Sch26e] Charles D. Schaper. *Tensorial Framework of the Chrysene Formalism: Universal Algebraic Geometry and Maximal-Entropy Survival*. Schaper Systems Press, San Francisco, CA, 2026. ISBN: 979-8-950371-03-5.

[Wäc90] Günter Wächtershäuser. Evolution of the first metabolic cycles. *Proceedings of the National Academy of Sciences*, 87(1):200–204, 1990.